

Impedances and Instabilities

R. Wanzenberg

Deutsches Elektronen-Synchrotron DESY, D-22603 Hamburg, Germany

Abstract

The concepts of wake fields and impedance are introduced to describe the electromagnetic interaction of a bunch of charged particles with its environment in an particle accelerator. The wake fields can act back on the beam and lead to instabilities, which may limit the achievable current per bunch, the total current, or even both. Some typical examples are used to illustrate the wake function and its basic properties. Then the frequency-domain view of the wake field or impedance is explained, and basic properties of the impedance are derived. The impedance of a cavity mode is illustrated using an equivalent circuit model. The relation of wake field effects to important beam parameters is treated in the rigid beam approximation. Several examples are employed to illustrate the impact of the geometry and the material properties of the vacuum chamber on the impedance. Finally, a basic introduction to beam instabilities based on a head tail model of the beam is given.

Keywords

Wake field; impedance; instabilities.

1 Introduction

A beam in an accelerator interacts with its vacuum chamber surroundings via electromagnetic fields. In this lecture the concept of wake fields is introduced to describe the electromagnetic interaction of a bunch of charged particles with its environment. The various components of the environment are the vacuum chamber, cavities, bellows, dielectric-coated pipes, and other kinds of obstacles the beam has to pass on its way through the accelerator. The wake fields can act back on the beam and lead to instabilities, which may limit the achievable current per bunch, the total current, or even both.

This lecture builds upon a previous lecture on wake fields and impedance given by T. Weiland [1] and M. Dohlus and the author [2]. Furthermore, there are excellent textbooks available [3–6] which cover the subject matter of this lecture.

In the introduction several typical examples are presented which demonstrate the interaction of a beam with the surrounding vacuum chamber via wake fields.

Then, in Section 2, the concept of wake potential is formally introduced and multipole expansions are studied for structures with cylindrical symmetry. The Panofsky–Wenzel theorem, which links the longitudinal and transverse wake forces, is explained.

Section 3 is devoted to the analysis of wake fields due to resonant modes in a cavity. The coupling of the beam to one mode of a cavity leads to the concept of the loss parameter.

In Section 4, the impedance is introduced as the Fourier transform of the wake potential. The properties of the wake functions (time-domain view) are translated to properties of the impedance (frequency-domain view).

1.1 Basic concepts

Consider a point charge q moving in free space at a velocity v close to the speed of light. The electromagnetic field is Lorentz-contracted into a thin disk perpendicular to the particle’s direction of motion [7],

which we choose to be the z -axis in a cylindrical coordinate system. The opening angle of the field distribution is of the order of $1/\gamma$, where $\gamma = (1 - (v/c)^2)^{-1/2}$. The field distribution is shown in Fig. 1. Even for an electron beam with an energy of $E = 10$ MeV, the opening angle ϕ is no greater than 50 mrad or 2.89° :

$$\phi = \frac{1}{\gamma} = \frac{0.511 \text{ MeV}}{E} = 2.89^\circ$$

($m_0 c^2 = 0.511$ MeV is the rest mass of the electron).

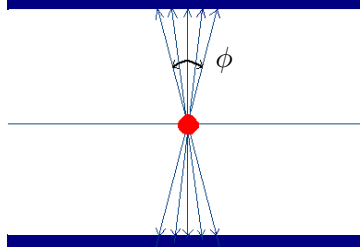


Fig. 1: Electromagnetic field carried by a relativistic point charge q

In the ultra-relativistic limit $v \rightarrow c$ (or $\gamma \rightarrow \infty$), the disk containing the field shrinks to a δ -function distribution. The non-vanishing field components are

$$E_r = \frac{q}{2\pi\epsilon_0 r} \delta(z - ct), \quad H_\phi = \frac{E_r}{Z_0} \quad \text{with } Z_0 = 377 \Omega.$$

Since the electric field \mathbf{E} points strictly radially outward from the point charge, all field components are identically zero both ahead of and behind the point charge, and hence there are no forces on a test particle either preceding or following the charge q .

For v slightly less than c , this is not strictly true. However, if we look at some typical bunch charges and energies of high-energy accelerators and synchrotron light sources, as shown in Table 1, we will notice that the space charge force $V_s = e/(4\pi\epsilon_0 d^2 \gamma^2)$ (where d is the rms distance between two electrons in the bunch) scales with $1/\gamma^2$. It is then obvious that as a good approximation, any space charge effects can be neglected for the accelerators under consideration. Nevertheless, space charge effects are important in heavy ion or low-energy proton accelerators.

Table 1: Typical bunch charges and energies of high-energy accelerators and synchrotron light sources [8–10]

Machine	Charge (nC)	Energy (GeV)	$\gamma = (1 - (v/c)^2)^{-1/2}$
LHC	20	7000	7 500
LEP	100	60	195 700
PETRA III	20	6	11 700

In the next section we will restrict ourselves to the ultra-relativistic case ($\gamma = \infty$, $v = c$), so space charge effects are neglected.

1.2 Some simple examples

Consider some typical settings where electromagnetic fields occur behind a bunch with charge q moving with velocity c through a structure. A bunch moves through a cylindrical pipe along the z -axis. All

electric field lines terminate transversely on surface charges on the wall of the pipe, assuming a perfectly conducting wall. There will be no wake fields behind the charge. The situation is different, however, if the cross-section of the beam pipe changes. A step-out transition is shown in Fig. 2. All fields have been calculated using a numerical wake field solver from MAFIA or the CST studio suite [11–14]. Here

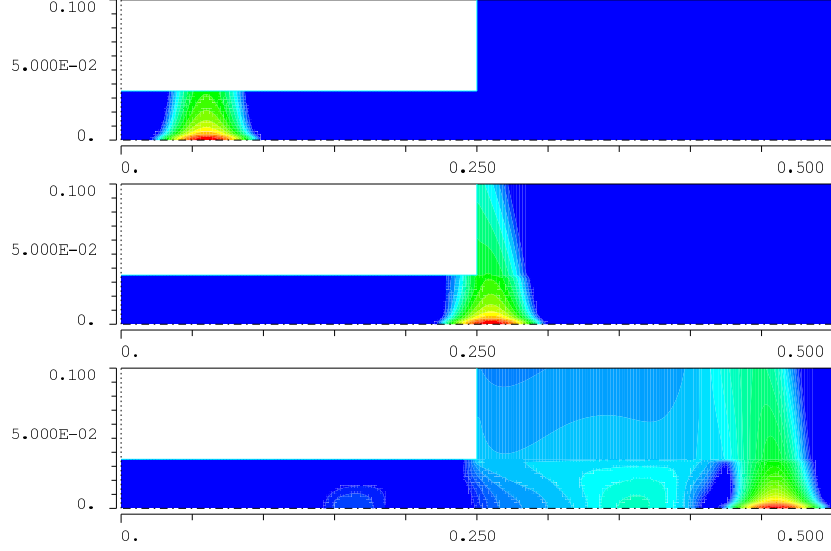


Fig. 2: Wake fields behind a bunch generated at a step-out transition from a small to a larger beam pipe

we have assumed that all pipe walls are perfect conductors. The wake field is generated because of the change in geometry. It should be noted that any beam pipe with finite conductivity, as well as flat beam pipes, can generate wake fields (resistive wall wake fields) [15]. Furthermore, a dielectric-coated pipe, which could be used as a travelling-wave acceleration section, will generate wake fields; see, for example, [16].

Another example is a cavity in a beam pipe; see Fig. 3. Again, a bunch is moving through a cylindrical pipe along the z -axis. Wake fields are generated because of geometrical changes in the pipe cross-section. In this respect the situation is similar to the previously considered case of a step-out transition. The main difference is that the bunch can excite modes in the cavity and therefore long-range wake fields, which can ring for a long time in the cavity (depending on the conductivity of the cavity wall).

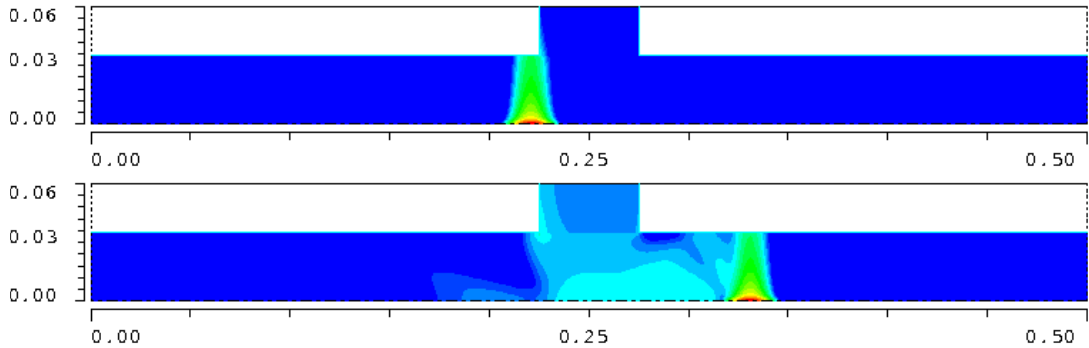


Fig. 3: Wake fields in a cavity

The examples have demonstrates that wake forces are caused by geometrical changes along the beam pipe. Space charge effects are negligible for ultra-relativistic particles. Wake fields due to the

resistive wall or dielectric coatings should always be checked in detail according to the specific situation. Furthermore, the surface roughness of the vacuum chamber can be important for special cases [17].

2 Wake fields

2.1 Wake fields in a resonant cavity with beam pipes

The examples above give us a qualitative understanding of wake fields and how they are generated. Before proceeding to mathematical descriptions in terms of wake potentials, let us take a closer look at the example considered in Section 1.

An ultra-relativistic point particle with charge q_1 traverses a small cavity parallel to the z -axis, with offset (x_1, y_1) ; see Fig. 4. The electromagnetic force on any test charge q_2 is given as a function of

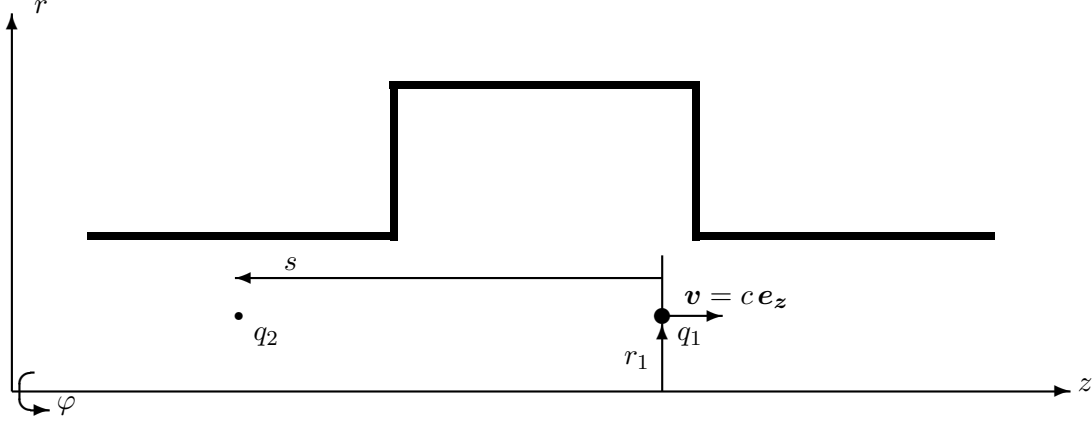


Fig. 4: An ultra-relativistic point particle with charge q_1 traverses a small cavity parallel to the z -axis, followed by a test charge q_2

space and time coordinates by the Lorentz equation

$$\mathbf{F}(\mathbf{r}, t) = q_2 (\mathbf{E}(\mathbf{r}, t) + \mathbf{v} \times \mathbf{B}(\mathbf{r}, t)),$$

where \mathbf{E} and \mathbf{B} are the fields generated by q_1 ; they are solutions of the Maxwell equations

$$\begin{aligned} \nabla \times \mathbf{B} &= \mu_0 \mathbf{j} + \frac{1}{c^2} \frac{\partial}{\partial t} \mathbf{E}, & \nabla \cdot \mathbf{B} &= 0, \\ \nabla \times \mathbf{E} &= -\frac{\partial}{\partial t} \mathbf{B}, & \nabla \cdot \mathbf{E} &= \frac{1}{\epsilon_0} \rho \end{aligned}$$

and have to satisfy several boundary conditions.

In our case the charge and current distributions are

$$\begin{aligned} \rho(\mathbf{r}, t) &= q_1 \delta(x - x_1) \delta(y - y_1) \delta(z - ct), \\ \mathbf{j}(\mathbf{r}, t) &= c \mathbf{e}_z \rho(\mathbf{r}, t). \end{aligned}$$

After interaction of q_1 with the cavity, there remain electromagnetic fields in the cavity. The source particle has lost energy to cavity modes and excited fields that propagate in the semi-infinite beam pipes.

Now consider a test charge q_2 following q_1 at a distance s with the same velocity $v \approx c$ and with offset (x_2, y_2) . The Lorentz force is

$$\mathbf{F}(x_1, y_1, x_2, y_2, s, t) = q_2 (\mathbf{E}(x_2, y_2, z = ct - s, t) + c \mathbf{e}_z \times \mathbf{B}(x_2, y_2, z = ct - s, t)).$$

The change in momentum of the test charge can be calculated as the time-integrated Lorentz force,

$$\Delta \mathbf{p}(x_1, y_1, x_2, y_2, s) = \int \mathbf{F} dt.$$

This leads to the concept of wake functions.

The electromagnetic fields \mathbf{E}_d and \mathbf{B}_d and the Lorentz Force \mathbf{F}_d of a distributed source $\rho_d(\mathbf{r}, t) = \eta(x_1 - \bar{x}_1, y_1 - \bar{y}_1)\lambda(z - ct)$ can be calculated either by integration over all source points,

$$\mathbf{F}_d(\bar{x}_1, \bar{y}_1, x_2, y_2, s, t) = \int \mathbf{F}(x_1, y_1, x_2, y_2, s, t + z_1/c) \eta(x_1 - \bar{x}_1, y_1 - \bar{y}_1) \frac{\lambda(z_1)}{q_1} dx_1 dy_1 dz_1,$$

or by solving the electromagnetic problem for the distributed source; here λ is the line charge density, η is the transverse distribution normalized to 1, and \bar{x}_1 and \bar{y}_1 describe a transverse shift of the center of the distribution. A calculation of the electric fields of a distributed source is shown in Fig. 5.

A fundamental difference between fields of point particles (with time dependency $\delta(z - ct)$) and fields of distributed sources (with time dependency $\lambda(z - ct)$) is that the frequency spectrum of point particles is not limited. In particular, long Gaussian bunches may stimulate only a few resonances (modes) in a cavity structure, or even none.

We can distinguish between the long-range regime of the wake, where the interaction between particles is driven by resonances, and the short-range regime, where the superposition of time-harmonic cavity fields is not sufficient to describe the effects. For instance, the fields in Fig. 2 are not determined by oscillations, while the fields in Fig. 5 will ring harmonically on one or several frequencies after the (source) bunch has left the domain.

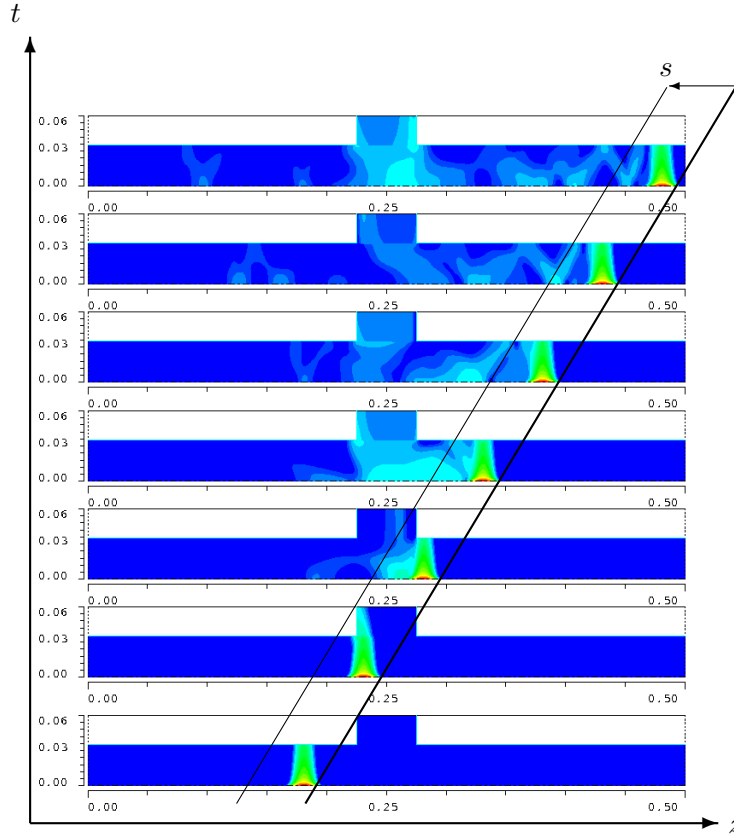


Fig. 5: Wake fields generated by a Gaussian bunch traversing a cavity

2.2 Basic definitions

Consider a point charge q_1 traversing a structure with offset (x_1, y_1) parallel to the z -axis at the speed of light (see Fig. 4). Then the *wake function* is defined as

$$\mathbf{w}(x_1, y_1, x_2, y_2, s) = \frac{1}{q_1} \int_{-\infty}^{\infty} dz [\mathbf{E}(x_2, y_2, z, t) + c \mathbf{e}_z \times \mathbf{B}(x_2, y_2, z, t)]_{t=(s+z)/c}.$$

The distance s is measured from the source q_1 in the opposite direction to \mathbf{v} . The change in momentum of a test particle with charge q_2 following behind at a distance s with offset (x_2, y_2) is given by

$$\Delta \mathbf{p} = \frac{1}{c} q_1 q_2 \mathbf{w}(s).$$

Since $\mathbf{e}_z \cdot (\mathbf{e}_z \times \mathbf{B}) = 0$, the longitudinal component of the wake function is simply

$$w_{\parallel}(x_1, y_1, x_2, y_2, s) = \frac{1}{q_1} \int_{-\infty}^{\infty} dz E_z(x_2, y_2, z, (s+z)/c).$$

Figure 6 shows the longitudinal component of the wake potential for the above example with the small cavity. The grey line represents the Gaussian charge distribution in the range from -5σ to 10σ . Owing to transient wake field effects, the head of the bunch (left-hand side of the figure) is decelerated, while a test charge at a certain position behind the bunch will be accelerated.

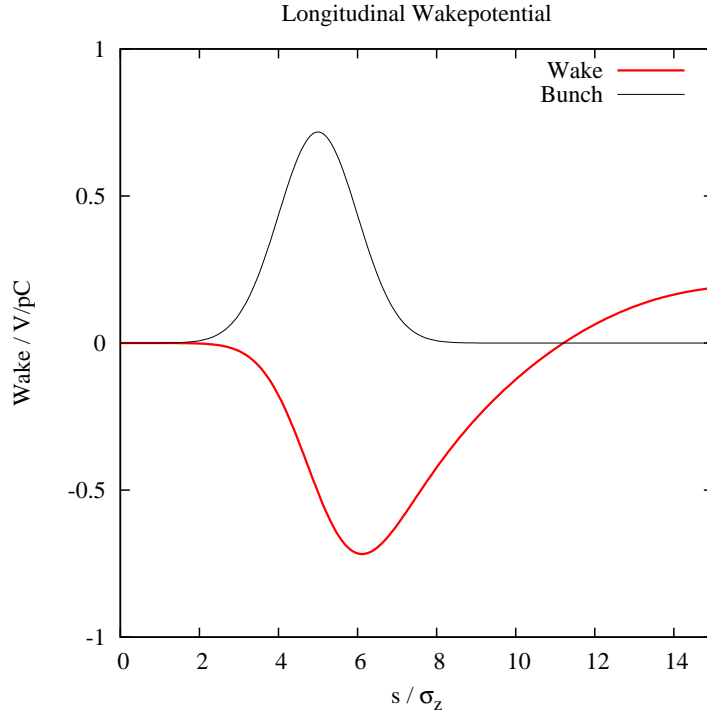


Fig. 6: Longitudinal wake potential

The notion of wakes, as presented above, is restricted to sources and test particles that travel at the velocity of light through a structure with semi-infinite input and output beam pipes. Therefore, for the integrals to converge, it is necessary that there be no length-independent forces in the pure beam pipes. This is the case for $v \rightarrow c$ and perfect conductivity of the pipes. The concept of a wake per length,

$$\mathbf{w}'(x_1, y_1, x_2, y_2, s) = \frac{1}{q_1} [\mathbf{E}_p(x_2, y_2, -s, 0) + v \mathbf{e}_z \times \mathbf{B}_p(x_2, y_2, -s, 0)],$$

is used to describe the effect in beam pipes ‘p’ of finite conductivity and/or velocity $v \leq c$. Suppose that the input and output beam pipes have the same cross-section; then a generalized wake function

$$\mathbf{w}_s(x_1, y_1, x_2, y_2, s) = \frac{1}{q_1} \int_{-\infty}^{\infty} dz [\mathbf{E}_s(x_2, y_2, z, t) + v \mathbf{e}_z \times \mathbf{B}_s(x_2, y_2, z, t)]_{t=(s+z)/v}$$

can be defined for the scattered fields $\mathbf{E}_s = \mathbf{E} - \mathbf{E}_p$ and $\mathbf{B}_s = \mathbf{B} - \mathbf{B}_p$. If the conditions for the wake function are fulfilled (i.e. convergence of the integral), then the wake function equals the generalized wake function.

The *wake potential* is defined similarly to the wake function, but for a distributed source:

$$\begin{aligned} \mathbf{W}(\bar{x}_1, \bar{y}_1, x_2, y_2, s) &= \frac{1}{q_1} \int_{-\infty}^{\infty} dz [\mathbf{E}_d(x_2, y_2, z, t) + c \mathbf{e}_z \times \mathbf{B}_d(x_2, y_2, z, t)]_{t=(s+z)/c} \\ &= \frac{1}{q_1 q_2} \int_{-\infty}^{\infty} dz [\mathbf{F}_d(\bar{x}_1, \bar{y}_1, x_2, y_2, z, t)]_{t=(s+z)/c}. \end{aligned}$$

It can be calculated from the wake function by the convolution

$$\mathbf{W}_d(\bar{x}_1, \bar{y}_1, x_2, y_2, s) = \int \mathbf{w}(x_1, y_1, x_2, y_2, s + z_1) \eta(x_1 - \bar{x}_1, y_1 - \bar{y}_1) \frac{\lambda(z_1)}{q_1} dx_1 dy_1 dz_1.$$

Note that the s -coordinate measures in the negative z -direction while λ depends on the positive longitudinal coordinate. Usually numerical codes for computing wakes, such as ECHO, calculate electromagnetic fields for distributed sources and therefore wake potentials.

2.3 Some theory

2.3.1 The Panofsky–Wenzel theorem

We follow the arguments of A. Chao [3, 18] to introduce the Panofsky–Wenzel theorem [19]. Therefore we use the following different notation for the generalized wake function:

$$\mathbf{w}_p(x_1, y_1, x_2, y_2, s) = \mathbf{w}_p(x_1, y_1, \mathbf{r}_2),$$

with the observer vector $\mathbf{r}_2 = x_2 \mathbf{e}_x + y_2 \mathbf{e}_y - s \mathbf{e}_z$. We calculate curl \mathbf{w}_p with respect to the observer or the test particle:

$$\nabla_2 \times \mathbf{w}_p(x_1, y_1, \mathbf{r}_2) = \nabla_2 \times \frac{v}{q_1} \int_{-\infty}^{\infty} dt [\mathbf{E}_s(\mathbf{r}_2 + \mathbf{v}t, t) + \mathbf{v} \times \mathbf{B}_s(\mathbf{r}_2 + \mathbf{v}t, t)].$$

Using curl $\mathbf{E} = -\partial \mathbf{B} / \partial t$ gives

$$\begin{aligned} \nabla_2 \times \mathbf{w}_p(x_1, y_1, \mathbf{r}_2) &= \frac{v}{q_1} \int_{-\infty}^{\infty} dt \left[-\frac{\partial}{\partial t} \mathbf{B}_s(\dots, t) + \mathbf{v}(\nabla_2 \mathbf{B}_s(\dots, t)) - \mathbf{B}_s(\dots, t)(\nabla_2 \mathbf{v}) \right] \\ &= \frac{v}{q_1} \int_{-\infty}^{\infty} dt \left[-\frac{\partial}{\partial t} - v \frac{\partial}{\partial z} \right] \mathbf{B}_s(\mathbf{r}_2 + \mathbf{v}t, t) \\ &= \frac{v}{q_1} \int_{-\infty}^{\infty} dt \left[-\frac{d}{dt} \mathbf{B}_s(\mathbf{r}_2 + \mathbf{v}t, t) \right] \\ &= -\frac{v}{q_1} \mathbf{B}_s(\mathbf{r}_2 + \mathbf{v}t, t) \Big|_{t=-\infty}^{t=\infty}. \end{aligned}$$

As the scattered field is zero for negative infinite time and vanishes for positive infinite time and infinite distance from the scattering object, the wake is curl-free. The Panofsky–Wenzel theorem is then reformulated in our original notation as the set of equations

$$\frac{\partial}{\partial s} w_{px} = -\frac{\partial}{\partial x_2} w_{p\parallel},$$

$$\begin{aligned}\frac{\partial}{\partial s} w_{py} &= -\frac{\partial}{\partial y_2} w_{p\parallel}, \\ \frac{\partial}{\partial x_2} w_{py} &= \frac{\partial}{\partial y_2} w_{px}.\end{aligned}$$

Note that the Panofsky–Wenzel theorem holds for the generalized wake function ($v \leq c$) and for the wake function ($v = c$).

Integration of the transverse gradient of the longitudinal wake function yields the transverse wake potential

$$\mathbf{w}_\perp(x_1, y_1, x_2, y_2, s) = -\nabla_{2\perp} \int_{-\infty}^s ds' w_\parallel(x_1, y_1, x_2, y_2, s').$$

The Panofsky–Wenzel theorem is applicable if the input and output beam pipes have the same cross-section.

2.3.2 Wake is harmonic with respect to observer offset

Now we calculate $\text{div } \mathbf{w}$ with respect to the observer. First, note that

$$\nabla_2 \cdot \mathbf{w}(x_1, y_1, \mathbf{r}_2) = \nabla_2 \cdot \frac{c}{q_1} \int_{-\infty}^{\infty} dt [\mathbf{E}(\mathbf{r}_2 + \mathbf{c}t, t) + \mathbf{c} \times \mathbf{B}(\mathbf{r}_2 + \mathbf{c}t, t)].$$

Using Maxwell's equations, $\text{div } \mathbf{E} = \rho/\varepsilon$ and $\text{curl } \mathbf{B} = \mu \mathbf{J} + c^{-2} \partial \mathbf{E} / \partial t$, together with $\mathbf{J} = c\rho$ gives

$$\begin{aligned}\nabla_2 \cdot \mathbf{w}(x_1, y_1, \mathbf{r}_2) &= \frac{c}{q_1} \int_{-\infty}^{\infty} dt [\nabla_2 \cdot \mathbf{E} + \mathbf{c}(\nabla_2 \times \mathbf{B})] \\ &= \frac{1}{q_1} \int_{-\infty}^{\infty} dt \left[-\frac{\partial}{\partial t} E_z(\mathbf{r}_2 + \mathbf{c}t, t) \right] \\ &= -\frac{1}{q_1} \int_{-\infty}^{\infty} dz \left[\frac{\partial}{\partial s} E_z(\mathbf{r}_2 + z\mathbf{e}_z, (z+s)/c) \right] \\ &= -\frac{\partial}{\partial s} w_\parallel(x_1, y_1, x_2, y_2, s).\end{aligned}$$

The term $\partial w_\parallel / \partial s$ appears on both sides of the equation, so we can write

$$\frac{\partial w_x}{\partial x_2} + \frac{\partial w_y}{\partial y_2} = 0.$$

With the Panofsky–Wenzel equations we find that the longitudinal wake is a harmonic function with respect to the transverse coordinates of the test particle:

$$\left(\frac{\partial^2}{\partial x_2^2} + \frac{\partial^2}{\partial y_2^2} \right) w_\parallel = -\frac{\partial}{\partial s} \left(\frac{\partial w_x}{\partial x_2} + \frac{\partial w_y}{\partial y_2} \right) = 0.$$

It is required that the trajectories (x_1, y_1, ct) and (x_2, y_2, ct) do not intersect with the boundary.

2.3.3 Wake is harmonic with respect to source offset

The longitudinal wake is also a harmonic function with respect to the transverse coordinates of the source particle [20], i.e. $L_1 w_\parallel = 0$ with $L_1 = \partial^2 / \partial x_1^2 + \partial^2 / \partial y_1^2$. To prove this, we have to calculate $\tilde{E}_z = L_1 E_z$, which is equivalent to the solution of the field problem for the source $\tilde{\rho} = L_1 \rho$. The source ρ is the point particle q_1 travelling at the speed of light along $(x_1, y_1, z = ct)$. It gives rise to the electromagnetic fields

$$\mathbf{E}_f = q_1 \frac{\delta(z - ct)}{2\pi\varepsilon} \frac{(x - x_1)\mathbf{e}_x + (y - y_1)\mathbf{e}_y}{(x - x_1)^2 + (y - y_1)^2},$$

$$\mathbf{B}_f = c^{-1} \mathbf{e}_z \times \mathbf{E}_f$$

in free space. The fields $\tilde{\mathbf{E}} = L_1 \mathbf{E}_f$ and $\tilde{\mathbf{B}} = L_1 \mathbf{B}_f$ are caused by the source $\tilde{\rho} = L_1 \rho$. These fields are zero for all points with $(x, y) \neq (x_1, y_1)$, as

$$\left(\frac{\partial^2}{\partial x_1^2} + \frac{\partial^2}{\partial y_1^2} \right) \frac{(x - x_1)\mathbf{e}_x + (y - y_1)\mathbf{e}_y}{(x - x_1)^2 + (y - y_1)^2} = \mathbf{0}.$$

Obviously $\tilde{\mathbf{E}}$ and $\tilde{\mathbf{B}}$ satisfy any linear boundary condition for any geometry, provided that the boundary does not intersect the trajectory $(x_1, y_1, z = ct)$. Therefore these fields are also solutions to the bounded wake problem, and all components of \mathbf{w} are harmonic with respect to (x_1, y_1) , since

$$\left(\frac{\partial^2}{\partial x_1^2} + \frac{\partial^2}{\partial y_1^2} \right) \mathbf{w} = \frac{c}{q_1} \int_{-\infty}^{\infty} dt [\tilde{\mathbf{E}} + \mathbf{c} \times \tilde{\mathbf{B}}] = \mathbf{0}.$$

This information will help us to evaluate the r -dependence of the wake function in cylindrical symmetric structures in the next subsection, and it will enable us to efficiently calculate the wake function in fully 3D structures.

2.4 Wake function in cylindrically symmetric structures

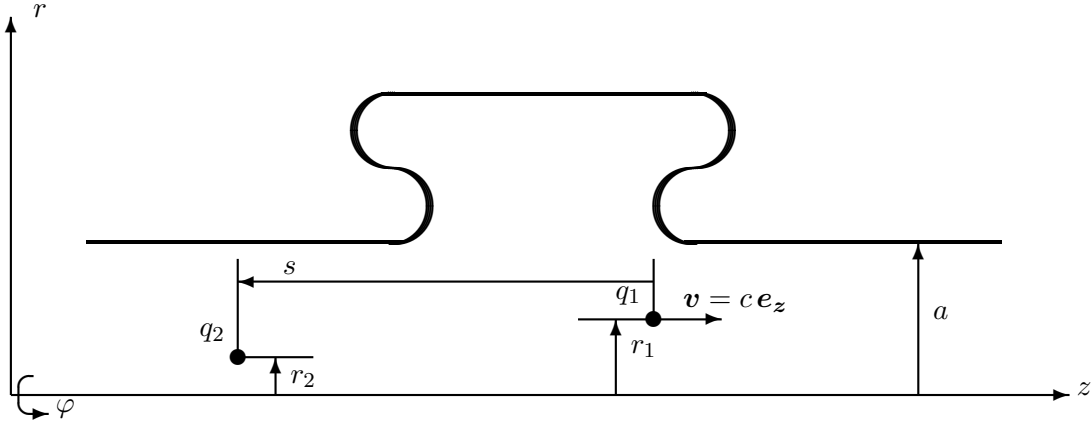


Fig. 7: A bunch with total charge q_1 traversing a cavity with offset r_1 , followed by a test charge q_2 with offset r_2

Consider now a cylindrically symmetric acceleration cavity with side tubes of radius a (see Fig. 7). The particular shape in the region $r > a$ is of no importance for the following investigations. Two charges pass through the structure from left to right with the speed of light: q_1 at a radius of r_1 and q_2 at a radius of r_2 . We wish to find an expression for the net change in momentum, $\Delta \mathbf{p}(r_1, \varphi_1, r_2, \varphi_2, s)$, experienced by q_2 due to the wake fields generated by q_1 . In the following we write the wake function and potential in polar coordinates. Let us start with the case of $\varphi_1 = 0$:

$$\Delta p_z(r_1, 0, r_2, \varphi_2, s) = q_1 q_2 w_{\parallel}(r_1, 0, r_2, \varphi_2, s).$$

The wake function can be expanded in a multipole series

$$w_{\parallel}(r_1, 0, r_2, \varphi_2, s) = \text{Re} \left\{ \sum_{m=-\infty}^{\infty} \exp(i m \varphi_2) G_m(r_1, r_2, s) \right\}.$$

Since w_{\parallel} is a harmonic function in (r_2, φ_2) , we have

$$\begin{aligned} L_2 w_{\parallel}(r_1, 0, r_2, \varphi_2, s) &= \left(\frac{1}{r_2} \frac{\partial}{\partial r_2} r_2 \frac{\partial}{\partial r_2} + \frac{1}{r_2^2} \frac{\partial^2}{\partial \varphi_2^2} \right) w_{\parallel}(r_1, 0, r_2, \varphi_2, s) \\ &= \operatorname{Re} \left\{ \sum_{m=-\infty}^{\infty} \exp(i m \varphi_2) \left(\frac{1}{r_2} \frac{\partial}{\partial r_2} r_2 \frac{\partial}{\partial r_2} - \frac{m^2}{r_2^2} \right) G_m(r_1, r_2, s) \right\} \\ &= 0, \end{aligned}$$

where L_2 is the transverse Laplace operator with respect to the offset of the test particle. So, for all m , the expansion functions $G_m(r_1, r_2, s)$ have to satisfy the Poisson equation

$$\frac{1}{r_2} \frac{\partial}{\partial r_2} \left(r_2 \frac{\partial}{\partial r_2} G_m(r_1, r_2, s) \right) - \frac{m^2}{r_2^2} G_m(r_1, r_2, s) = 0.$$

The solutions are

$$\begin{aligned} G_0(r_1, r_2, s) &= U_0(r_1, s) + V_0(r_1, s) \ln r_2, \\ G_m(r_1, r_2, s) &= U_m(r_1, s) r_2^m + V_m(r_1, s) r_2^{-m} \quad \text{for } m > 0. \end{aligned}$$

Keeping only the solutions which are regular at the origin ($r_2 = 0$), the longitudinal wake potential can be written as

$$w_{\parallel}(r_1, 0, r_2, \varphi_2, s) = \sum_{m=0}^{\infty} r_2^m U_m(r_1, s) \cos m \varphi_2,$$

with expansion functions $U_m(r_1, s)$ that depend on the details of the given cavity geometry.

By azimuthal symmetry, the dependence on φ_1 is $w_{\parallel}(r_1, \varphi_1, r_2, \varphi_2, s) = w_{\parallel}(r_1, 0, r_2, \varphi_2 - \varphi_1, s)$, as longitudinal fields depend only on the relative azimuthal angle of the observer with respect to the source. Using the fact that w_{\parallel} is also a harmonic function in (r_1, φ_1) , we find with the same arguments as before that $U_m(r_1, s)$ can be factorized as $r_1^m w_m(s)$.

It follows that for the general case of a charge q_1 at (r_1, φ_1) generating fields that act on a second charge q_2 at (r_2, φ_2) , the *longitudinal wake function* is given by

$$w_{\parallel}(r_1, \varphi_1, r_2, \varphi_2, s) = \sum_{m=0}^{\infty} r_1^m r_2^m w_m(s) \cos m(\varphi_2 - \varphi_1).$$

The transverse wake function is, by the Panofsky–Wenzel theorem,

$$\begin{aligned} \mathbf{w}_{\perp}(r_1, \varphi_1, r_2, \varphi_2, s) &= - \left(\mathbf{e}_r \frac{\partial}{\partial r_2} + \mathbf{e}_{\varphi} \frac{1}{r_2} \frac{\partial}{\partial \varphi_2} \right) \int_{-\infty}^s ds' w_{\parallel}(r_1, \varphi_1, r_2, \varphi_2, s') \\ &= \sum_{m=0}^{\infty} \left\{ -\mathbf{e}_r m r_1^m r_2^{m-1} \int_{-\infty}^s ds' w_m(s') \cos m(\varphi_2 - \varphi_1) \right. \\ &\quad \left. + \mathbf{e}_{\varphi} m r_1^m r_2^{m-1} \int_{-\infty}^s ds' w_m(s') \sin m(\varphi_2 - \varphi_1) \right\}. \end{aligned}$$

Each azimuthal order is fully characterized by a scalar function $w_m(s)$. This function can be calculated by solving Maxwell's equations for the given geometry and any choice of $(r_1, \varphi_1, r_2, \varphi_2)$, yielding

$$w_m(s) = \frac{\int_{-\infty}^{\infty} dz E_{zm}(r_2, \varphi_2, z, (z + s)/c)}{r_1^m r_2^m \cos m(\varphi_2 - \varphi_1)}.$$

A particular choice of r_2 can be used to avoid the infinite integration range: since E_z vanishes at the metallic tube boundary, only the cavity gap contributes to the integral. The integration range is reduced to the cavity gap by setting r_2 to the radius of the beam tube. This trick is possible if no obstacle intersects with the infinite cylindrical beam pipe.

This type of wake integration is utilized by computer codes such as ECHO [21,22] for bunches of finite length. Wake potentials can be calculated by such programs in the time domain, but wake functions (of point sources) need asymptotic considerations; see [23].

It should be mentioned that in many practical cases, due to the $(r/a)^m$ dependence, the longitudinal wake is dominated by the monopole term and the transverse wakes by the dipole term:

$$w_{\parallel}(r_1, \varphi_1, r_2, \varphi_2, s) = w_0(s),$$

$$w_{\perp}(r_1, \varphi_1, r_2, \varphi_2, s) = r_1 \int_{-\infty}^s ds' w_1(s') [-\mathbf{e}_r \cos(\varphi_2 - \varphi_1) + \mathbf{e}_{\varphi} \sin(\varphi_2 - \varphi_1)].$$

2.5 Fully 3D structures

While for cylindrical symmetric structures the dependence of the wake on transverse coordinates is explicitly known and can be used to reduce the integration range and domain of the field calculation, more general structures require us to use the harmonic property of the wake for a beam tube of arbitrary shape. The simple 3D cavity in Fig. 8, with a beam tube of square cross-section, is used to demonstrate this. We suppress the dependence of the wake function (or potential) on the offset of the source and write simply $\tilde{W}_{\parallel}(x, y, s) = W_{\parallel}(x_1, y_1, x, y, s)$. This function is harmonic in the observer offset,

$$\nabla_{\perp}^2 \tilde{W}_{\parallel}(x, y, s) = 0.$$

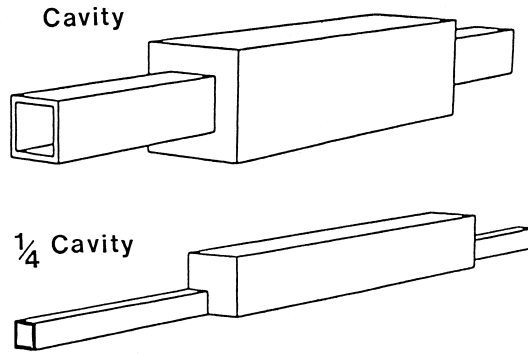


Fig. 8: A 3D cavity structure with two symmetry planes (top) and a quarter of the structure (bottom)

For points x and y on the surface of the beam tube, we can calculate the wake by a finite-range integration through the cavity gap, as shown in Fig. 9. If we know \tilde{W} for all surface points, we can calculate the wake for any point inside the tube by numerical solution of the boundary value problem. Therefore a 2D Poisson problem has to be solved. In our example, with two transverse symmetries, only a quarter of the structure needs to be considered to calculate the wake of a source in the center.

The transverse wake potential can be calculated from the longitudinal one using the Panofsky–Wenzel theorem. The transverse gradient of the longitudinal wake potential in a beam tube is also indicated in Fig. 9.

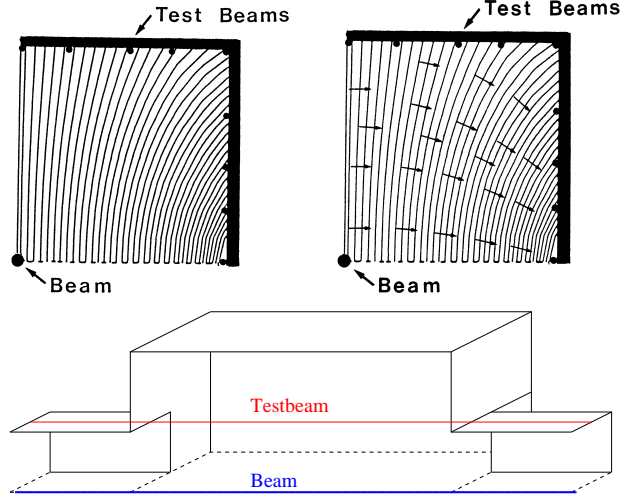


Fig. 9: Illustration of the indirect test beam method. The upper pictures show lines of constant longitudinal wake potential and the gradient of the longitudinal wake potential; an integration gives the transverse wake potential according to the Panofsky–Wenzel theorem. The lower diagram depicts the paths of the beam and the test beam.

3 Cavities, resonant structures and eigenmodes

3.1 Eigenmodes

Many structures in an accelerator environment can be considered as a hollow space with semi-infinite beam pipes on both sides. Usually this vacuum volume is bounded by metal surfaces with high conductivity. As a good approximation, the cavity walls can be treated as perfect electric conducting (PEC) boundaries, and sometimes the beam pipes are even neglected so that the volume is closed.

Electromagnetic fields with frequencies below the lowest cutoff frequency of the beam pipes are trapped in the volume, and the fields oscillate at discrete frequencies:

$$\begin{aligned} \mathbf{E}(\mathbf{r}, t) &= \sum_{\nu} \hat{A}_{\nu} \hat{\mathbf{E}}_{\nu}(\mathbf{r}) \cos(\hat{\omega}_{\nu} t + \hat{\varphi}_{\nu}), \\ \mathbf{B}(\mathbf{r}, t) &= \sum_{\nu} \hat{A}_{\nu} \hat{\mathbf{B}}_{\nu}(\mathbf{r}) \sin(\hat{\omega}_{\nu} t + \hat{\varphi}_{\nu}). \end{aligned}$$

These oscillations are called eigenmodes or cavity modes. They are characterized by their field patterns $\hat{\mathbf{E}}_{\nu}(\mathbf{r})$ and $\hat{\mathbf{B}}_{\nu}(\mathbf{r})$ and their eigenfrequencies $\hat{\omega}_{\nu}$. The modes may ring with any amplitude \hat{A}_{ν} and phase $\hat{\varphi}_{\nu}$, and the amplitude normalization of the eigenfields is arbitrary. Such modes are called standing-wave modes, as the electric and magnetic fields ring at all spatial points with the same phase, but the electric field is phase-shifted by 90° relative to the magnetic field. For simplicity, in the following we omit the mode index ν but indicate all indexable (mode-specific) quantities with a hat. We will introduce further mode-specific quantities, such as the quality \hat{Q} , the modal longitudinal loss parameter \hat{k} , and the mode energy

$$\hat{\mathcal{W}} = \frac{1}{2} \int \varepsilon \hat{E}^2 dV = \frac{1}{2} \int \mu^{-1} \hat{B}^2 dV,$$

which depends on the arbitrary amplitude normalization. The total electromagnetic field energy of all the modes is¹

$$\mathcal{W} = \frac{1}{2} \int \varepsilon E(\mathbf{r}, t)^2 dV + \frac{1}{2} \int \mu^{-1} B(\mathbf{r}, t)^2 dV = \sum |\hat{A}|^2 \hat{\mathcal{W}}.$$

¹The field energy of a particular mode does not depend on the stimulation of other modes, as the mode fields are orthogonal to each other; see Appendix A.

Eigenmodes can be computed with electromagnetic field solvers such as those in [11, 12]; see also Fig. 10. Usually closed volumes are considered, which are completely surrounded by PEC or perfect magnetic conducting (PMC) surfaces. As the mode field in beam pipes decays exponentially, even open problems (involving infinitely long pipes) can be handled with such programs, by using a perfectly conducting boundary after a sufficiently long piece of pipe.

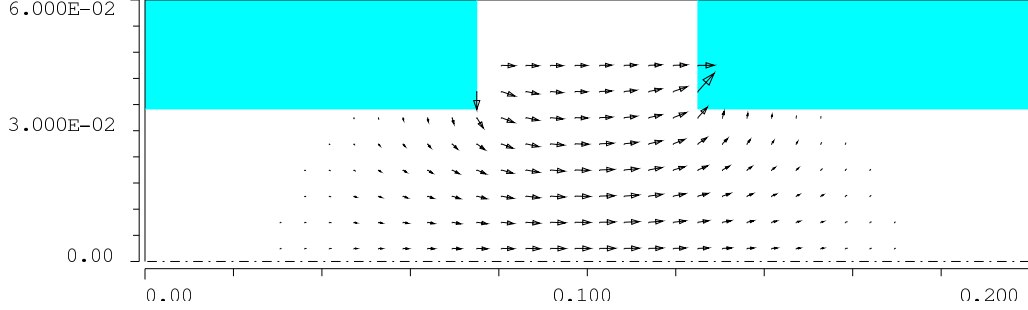


Fig. 10: Electric field of a mode in a rotationally symmetric cavity with beam pipes

In structures with symmetries (e.g. rotational symmetry), eigenmodes and beam-pipe modes of the same symmetry condition are coupled. Therefore the lowest cutoff frequency for a particular symmetry defines the highest possible eigenfrequency for the corresponding eigenmodes. For instance, monopole modes may have resonance frequencies that are above the lowest dipole mode cutoff frequency, which is lower than the lowest monopole mode cutoff frequency. Beyond that, there can exist quasi-trapped modes above the lowest cutoff frequency that have very weak coupling to the pipes. The energy flow (per period) of such fields into the beam pipes may be comparable to the energy loss (per period) of non-trapped modes to non-perfectly conducting metallic boundaries.

3.2 Excitation of eigenmodes and the per-mode loss parameter

We consider a cavity of length² L and a bunch with charge q_1 , offset (x_1, y_1) and velocity c , which enters the cavity at time $t = 0$. The electromagnetic fields after the charge has left the cavity, namely

$$\begin{aligned} \mathbf{E}(\mathbf{r}, t > L/c) &= \sum \text{Re}\{\hat{A}\hat{\mathbf{E}}(\mathbf{r}) \exp(i\hat{\omega}t)\} + \mathbf{E}_r(\mathbf{r}, t), \\ \mathbf{B}(\mathbf{r}, t > L/c) &= \sum \text{Im}\{\hat{A}\hat{\mathbf{B}}(\mathbf{r}) \exp(i\hat{\omega}t)\} + \mathbf{B}_r(\mathbf{r}, t), \end{aligned}$$

can be split into eigenfields and a residual part, \mathbf{E}_r or \mathbf{B}_r . The long-range interaction between bunches or particles is essentially driven by the modal part, as the residual fields decay or are not stimulated resonantly. The complex mode amplitudes are proportional to the source charge and depend on the source offset. Hence they can be expressed as $\hat{A} = q_1 \hat{f}(x_1, y_1)$.

Suppose that a small test charge δq follows the source particle on the same trajectory at a distance of $s > 0$. It induces the additional amplitude $\delta\hat{A} = \delta q \exp(-i\hat{\omega}s/c) \hat{f}(x_1, y_1)$. Therefore the energy of the modes is increased by

$$\begin{aligned} \delta\mathcal{W}_{\text{modes}} &= \sum (|\hat{A} + \delta\hat{A}|^2 - |\hat{A}|^2) \hat{\mathcal{W}} \\ &\approx \sum 2 \text{Re}\{\hat{A}\delta\hat{A}^*\} \hat{\mathcal{W}} \\ &\approx 2q_1\delta q \sum |\hat{f}(x_1, y_1)|^2 \text{Re}\{\exp(i\hat{\omega}s/c)\} \hat{\mathcal{W}}. \end{aligned}$$

²The relevant length is not exactly the length of the cavity, but rather the length with non-zero field of the modes. For open structures, with beam pipes, this length is in principle infinite, but for practical considerations the field has decayed sufficiently after a pipe length of a few times the widest dimension of the cross-section.

On the other hand, the test particle gains kinetic energy

$$\begin{aligned}\delta\mathcal{W}_k &= \int_{-\infty}^{\infty} \delta q E_z(x_1, y_1, z - s, z/c) dz \\ &= q_1 \delta q \sum \operatorname{Re} \left\{ \hat{f}(x_1, y_1) \int_{-\infty}^{\infty} \hat{E}_z(x_1, y_1, z) \exp(i\hat{\omega}(z + s)/c) dz \right\} + \dots\end{aligned}$$

The sum of the field energy and the kinetic energy is conserved, if terms with the same oscillation frequency $\exp(i\hat{\omega}s/c)$ cancel:

$$2|\hat{f}(x_1, y_1)|^2 \hat{\mathcal{W}} + \hat{f}(x_1, y_1) \int_{-\infty}^{\infty} \hat{E}_z(x_1, y_1, z) \exp(i\hat{\omega}(z)/c) dz = 0.$$

This is satisfied with $\hat{f}(x_1, y_1) = -\hat{v}^*(x_1, y_1)/\sqrt{\hat{\mathcal{W}}}$ and the normalized mode voltages

$$\hat{v}(x, y) = \frac{1}{2\sqrt{\hat{\mathcal{W}}}} \int_{-\infty}^{\infty} \hat{E}_z(x, y, z) \exp(i\hat{\omega}z/c) dz,$$

which do not depend on the arbitrary normalization mode fields.

The amplitude excited by the charge q_1 is

$$\hat{A} = q_1 \hat{f}(x_1, y_1) = -q_1 \hat{v}^*(x_1, y_1) / \sqrt{\hat{\mathcal{W}}},$$

and the energy of all modes is

$$\mathcal{W}_{\text{EM, modes}} = \sum |\hat{A}|^2 \hat{\mathcal{W}} = q_1^2 \sum \hat{k},$$

with the per-mode loss parameter

$$\hat{k} = |\hat{v}(x_1, y_1)|^2 = \frac{1}{4\hat{\mathcal{W}}} \left| \int_{-\infty}^{\infty} \hat{E}_z(x_1, y_1, z) \exp(i\hat{\omega}(z)/c) dz \right|^2.$$

The excitation of mode amplitudes depends linearly on the source distribution: another particle with charge q_2 and offset (x_2, y_2) at a distance s gives rise to the additional amplitude

$$\hat{A} = -q_2 \hat{v}^*(x_2, y_2) \exp(-i\hat{\omega}s/c) / \sqrt{\hat{\mathcal{W}}},$$

with phase shift $-\hat{\omega}s/c$ due to the time shift s/c . Therefore it is possible to calculate the mode excitation for arbitrary charge distributions; for example, for a one-dimensional bunch with offset (x_1, y_1) and line charge density $\lambda(z, t) = \lambda(z - ct)$,

$$\hat{A} = \hat{v}^*(x_1, y_1) \int \lambda(-s) \exp(-i\hat{\omega}s/c) ds.$$

In particular, a Gaussian bunch with charge q_1 and rms length σ excites the amplitudes $\hat{A} = q_1 \hat{v}^*(x_1, y_1) \exp(-(\hat{\omega}\sigma/c)^2/2)$. We introduce the shape-dependent per-mode loss parameter

$$\hat{k}_\sigma = \hat{k} \exp(-(\hat{\omega}\sigma/c)^2).$$

The electromagnetic field energy of all modes, after such a bunch has traversed the cavity, is

$$\mathcal{W}_{\text{EM, modes}, \sigma} = \sum |\hat{A}|^2 \hat{\mathcal{W}} = q_1^2 \sum \hat{k}_\sigma.$$

3.3 Contribution of eigenmodes to the wake function

After the source particle has traversed the cavity, the electromagnetic fields are

$$\begin{aligned}\mathbf{E}(\mathbf{r}, t > L/c) &= q_1 \sum \text{Re} \left\{ -\hat{v}^*(x_1, y_1) \hat{\mathcal{W}}^{-1/2} \hat{\mathbf{E}}(\mathbf{r}) \exp(i\hat{\omega}t) \right\} + \mathbf{E}_r(\mathbf{r}, t), \\ \mathbf{B}(\mathbf{r}, t > L/c) &= q_1 \sum \text{Im} \left\{ -\hat{v}^*(x_1, y_1) \hat{\mathcal{W}}^{-1/2} \hat{\mathbf{B}}(\mathbf{r}) \exp(i\hat{\omega}t) \right\} + \mathbf{B}_r(\mathbf{r}, t),\end{aligned}$$

Therefore the momentum of a test charge q_2 at a distance $s > L$ behind the source, with offset (x_2, y_2) and velocity c , is changed by

$$\Delta \mathbf{p} = \frac{q_1 q_2}{c} \sum \text{Re} \left\{ -\hat{v}^*(x_1, y_1) \hat{\mathcal{W}}^{-1/2} \int_{-\infty}^{\infty} dz \left[(\hat{\mathbf{E}} - i\mathbf{c} \times \hat{\mathbf{B}}) \exp(i\hat{\omega}(z+s)/c) \right] \right\} + \Delta \mathbf{p}_r,$$

where the term $\Delta \mathbf{p}_r$ stands for the contribution of the residual fields. Likewise, we can split the wake into modal and residual parts:

$$\mathbf{w}(x_1, y_1, x_2, y_2, s > L) = \frac{c\Delta \mathbf{p}}{q_1 q_2} = \sum \hat{\mathbf{w}}(x_1, y_1, x_2, y_2, s) + \mathbf{w}_r(x_1, y_1, x_2, y_2, s),$$

where

$$\hat{\mathbf{w}}(x_1, y_1, x_2, y_2, s > L) = -2 \text{Re} \left\{ \hat{v}^*(x_1, y_1) \hat{\mathbf{v}}(x_2, y_2) \exp(i\hat{\omega}s/c) \right\},$$

with the normalized vectorial voltages

$$\hat{\mathbf{v}}(x, y) = \frac{1}{2\sqrt{\hat{\mathcal{W}}}} \int_{-\infty}^{\infty} dz \left[(\hat{\mathbf{E}}(x, y, z) - i\mathbf{c} \times \hat{\mathbf{B}}(x, y, z)) \exp(i\hat{\omega}z/c) \right].$$

3.4 Loss parameters

Loss parameters describe the loss of energy of a source particle or source distribution to electromagnetic field energy.

We have seen that the total energy loss of a point particle is given by the wake function for $x_1 = x_2$, $y_1 = y_2$ and $s = 0$, so that

$$k_{\text{tot}} = -w(x_1, y_1, x_2, y_2, 0) = \mathcal{W}_{\text{EM}, \text{total}}/q_1,$$

and we know that the loss to eigenmodes is given by the per-mode loss parameters

$$\hat{k} = |v(x_1, y_1)|^2.$$

The sum of all the per-mode loss parameters converges for cavities *with* beam pipes to a value below the total loss parameter k_{tot} , as not only are there modes excited, but also field energy is scattered and propagates along the beam pipes. (The wake of a closed cavity is completely determined by oscillating modes, but the sum is divergent.)

The wake potential (of distributed sources) and the shape-dependent loss parameter are usually calculated directly using electromagnetic time-domain solvers. The shape-dependent total loss parameter is the convolution of the longitudinal wake potential with the charge density function; for instance, for bunches with longitudinal profile $\lambda(z, t) = \lambda(z - ct)$ and negligible transverse dimensions,

$$k_{\text{tot}, \sigma} = - \int_{-\infty}^{\infty} W(x_1, y_1, x_1, y_1, z) \lambda(z) dz.$$

The excitation of eigenmodes by distributed sources was discussed in Section 3.2; the shape-dependent per-mode loss parameter for a thin Gaussian bunch is

$$\hat{k}_\sigma = \hat{k} \exp(-(\hat{\omega}\sigma/c)^2),$$

and for a general longitudinal profile λ it is

$$\hat{k}_\sigma = \hat{k} \left| \int_{-\infty}^{\infty} \lambda(z) \cos(\hat{\omega}z/c) dz \right|^2.$$

For closed cavities, the sum of the per-mode loss parameters \hat{k}_σ converges to the total loss parameter $k_{\text{tot},\sigma}$. This is also true for long bunches with $\sigma \gg c/\omega_{\text{cutoff}}$, which cannot excite frequencies above the lowest cutoff frequency $\omega_{\text{cutoff}} \propto \pi c/a$ of the beam pipes, where a is the characteristic transverse dimension of the pipes.

For the extreme case of ultra-short bunches it is difficult to calculate the wake potential, as a very high spatial resolution is required. In this case, only a small fraction of energy is lost to resonant modes and only a small part of the wakes is caused by resonances.

4 Impedances

4.1 Definitions

The Fourier transform of the negative³ wake function is called the impedance or coupling-impedance:

$$Z_{\parallel}(x_1, y_1, x_2, y_2, \omega) = -\frac{1}{c} \int_{-\infty}^{\infty} ds w_{\parallel}(x_1, y_1, x_2, y_2, s) \exp(-i\omega s/c).$$

The wake function and impedance are two descriptions of the same thing, namely the coupling between the beam and its environment. The wake function is the time-domain description, while the impedance is the frequency-domain description:

$$w_{\parallel}(x_1, y_1, x_2, y_2, s) = -\frac{1}{2\pi} \int_{-\infty}^{\infty} d\omega Z_{\parallel}(x_1, y_1, x_2, y_2, \omega) \exp(i\omega s/c).$$

The reason for the usefulness of the impedance is that it often contains a number of sharply defined frequencies corresponding to the modes of the cavity or the long-range part of the wake. Figure 11 shows the real part of the impedance for a cavity. Below the cutoff frequency of the beam pipe, there is a sharp peak for each cavity mode. The spectrum above the cutoff frequency is continuous, caused by residual fields (not related to eigenmodes) and by the ‘turn-on’ of the harmonic eigen-oscillations. The continuous part of the spectrum is important for short-range wakes, especially for very short bunches.

For the transverse impedance, it is often convenient to use a definition containing an extra factor i :

$$\mathbf{Z}_{\perp}(x_1, y_1, x_2, y_2, \omega) = \frac{i}{c} \int_{-\infty}^{\infty} ds \mathbf{w}_{\perp}(x_1, y_1, x_2, y_2, s) \exp(-i\omega s/c).$$

The reason is that the transverse–longitudinal relations due to the Panofsky–Wenzel theorem then read as follows in the frequency domain:

$$\frac{\omega}{c} \mathbf{Z}_{\perp}(x_1, y_1, x_2, y_2, \omega) = \left(\mathbf{e}_x \frac{\partial}{\partial x_2} + \mathbf{e}_y \frac{\partial}{\partial y_2} \right) Z_{\parallel}(x_1, y_1, x_2, y_2, \omega).$$

³The sign is chosen so as to obtain a non-negative real part for $x_1 = x_2$ and $y_1 = y_2$.

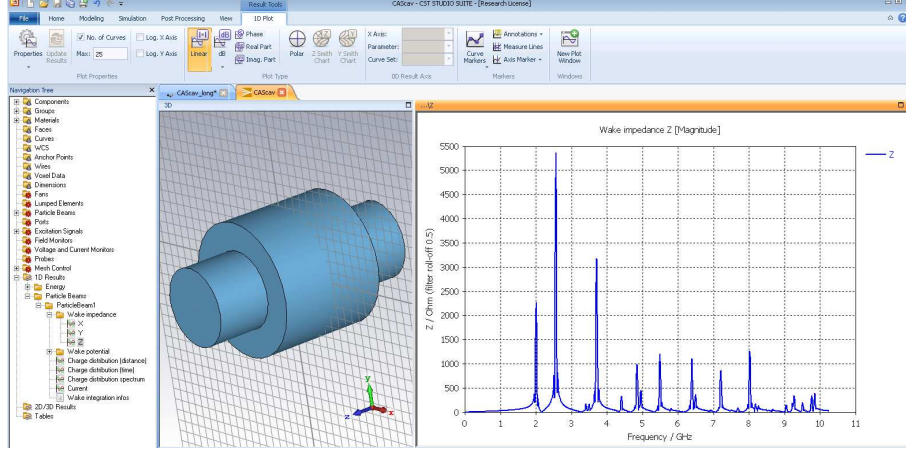


Fig. 11: Real part of the impedance for a cavity with side pipes; the peaks correspond to cavity modes. The results were obtained with the CST wakefield solver.

4.2 Some properties of impedances and wakes

In the spatial s -domain, the relationship between the wake potential of a line charge density $\lambda(z - ct)$ and the wake functions of a point particle is described by the convolution

$$W(x_1, y_1, x_2, y_2, s) = \int_{-\infty}^{\infty} dz w(x_1, y_1, x_2, y_2, s + z) \lambda(z).$$

The corresponding equation in the frequency domain for the Fourier transform of the negative wake potential is $V(x_1, y_1, x_2, y_2, \omega) = Z_{\parallel}(x_1, y_1, x_2, y_2, \omega) I(\omega)$, where

$$I(\omega) = \int_{-\infty}^{\infty} i(t) \exp(-i\omega t) dt = \int_{-\infty}^{\infty} c\lambda(-ct) \exp(-i\omega t) dt$$

is the beam current in the frequency domain. The energy loss of the bunch to electromagnetic fields,

$$\begin{aligned} \mathcal{W}_{\text{loss}} &= \int_{-\infty}^{\infty} W(x_1, y_1, x_1, y_1, s) \lambda(-s) ds \\ &= \frac{1}{2\pi} \int_{-\infty}^{\infty} V(x_1, y_1, x_1, y_1, \omega) I(\omega)^* d\omega \\ &= \frac{1}{\pi} \int_0^{\infty} \text{Re}\{Z(x_1, y_1, x_1, y_1, \omega)\} |I(\omega)|^2 d\omega, \end{aligned}$$

has to be non-negative for any bunch shape λ . Therefore the real part of the longitudinal impedance must be non-negative for all offsets with $x_1 = x_2$ and $y_1 = y_2$. The real part can be negative for, say, $x_1 = -x_2$ and $y_1 = -y_2$, for a structure with azimuthal symmetry and frequency close to a dipole resonance.

As the wake potential is a real function, the real part of the impedance is an even function of the frequency while the imaginary part is an odd function of it:

$$\text{Re}\{Z_{\parallel}(\dots, \omega)\} = \text{Re}\{Z_{\parallel}(\dots, -\omega)\}, \quad \text{Im}\{Z_{\parallel}(\dots, \omega)\} = -\text{Im}\{Z_{\parallel}(\dots, -\omega)\}.$$

Hence, the wake function is given in terms of the impedance as

$$w_{\parallel}(\dots, s) = -\frac{1}{2\pi} \int_{-\infty}^{\infty} d\omega Z_{\parallel}(\dots, \omega) \exp(i\omega s/c)$$

$$= -\frac{1}{2\pi} \int_{-\infty}^{\infty} d\omega \left(\operatorname{Re}\{Z_{\parallel}(\dots, \omega)\} \cos(\omega s/c) - \operatorname{Im}\{Z_{\parallel}(\dots, \omega)\} \sin(\omega s/c) \right).$$

Furthermore, the electromagnetic field ahead of the source particle is zero for $v = c$, as electromagnetic waves cannot overtake the source. Therefore, the wake function is *causal*, and the real and imaginary parts of the impedance are dependent on each other. From $w_{\parallel}(\dots, s < 0) = 0$ it follows that for $u = -s > 0$,

$$\int_{-\infty}^{\infty} d\omega \operatorname{Re}\{Z_{\parallel}(\dots, \omega)\} \cos(\omega u/c) = - \int_{-\infty}^{\infty} d\omega \operatorname{Im}\{Z_{\parallel}(\dots, \omega)\} \sin(\omega u/c),$$

so only the real (or imaginary) part of the impedance is really needed:

$$w_{\parallel}(\dots, s > 0) = \frac{1}{\pi} \int_{-\infty}^{\infty} d\omega \operatorname{Re}\{Z_{\parallel}(\dots, \omega)\} \cos(\omega s/c).$$

4.3 Shunt impedance and quality factor

The modal part of the wake function is

$$\hat{w}(x_1, y_1, x_2, y_2, s) = -2 \operatorname{Re}\{\hat{v}^*(x_1, y_1) \hat{v}(x_2, y_2) \exp(i \hat{\omega} s/c)\} \begin{cases} 0 & \text{for } s < 0, \\ 1 & \text{for } s = 0, \\ 2 & \text{otherwise.} \end{cases}$$

We are interested in the longitudinal component on the axis ($x_1 = y_1 = x_2 = y_2 = 0$), and for simplicity we omit the transverse coordinates, so

$$\hat{w}_{\parallel}(s) = -2\hat{k} \cos(\hat{\omega} s/c) \begin{cases} 0 & \text{for } s < 0, \\ 1 & \text{for } s = 0, \\ 2 & \text{otherwise.} \end{cases}$$

Then the impedance per mode,

$$\hat{Z}_{\parallel}(\omega) = -\frac{1}{c} \int_{-\infty}^{\infty} \hat{w}_{\parallel}(s) \exp(-i \omega s/c) ds,$$

is calculated as

$$\hat{Z}_{\parallel}(\omega) = 2\hat{k} \left\{ \pi \delta(\omega + \hat{\omega}) + \pi \delta(\omega - \hat{\omega}) + \frac{i \omega}{\hat{\omega}^2 - \omega^2} \right\}.$$

This is equivalent to the impedance of a parallel resonant circuit (see Fig. 12),

$$\hat{Z}_{\parallel}(\omega) = \lim_{\hat{R} \rightarrow \infty} \left(i \omega \hat{C} + \frac{1}{i \omega \hat{L}} + \frac{1}{\hat{R}} \right)^{-1}$$

with $\hat{C} = 1/(2\hat{k})$, $\hat{L} = 2\hat{k}/\hat{\omega}^2$ and $\hat{R} \rightarrow \infty$.

Although the resistor \hat{R} was introduced for obvious formal reasons, it is helpful to consider weak losses of a resonator with a high quality factor $\hat{Q} = \hat{R}/(\hat{\omega} \hat{L})$. The impedance per mode of a resonator with weak losses is

$$\hat{Z}_{\parallel}(\omega) = 2\hat{k} \frac{i \omega}{\hat{\omega}^2 - \omega^2 + i \omega \hat{\omega} / \hat{Q}}.$$

The resistor $R = \hat{Z}_{\parallel}(\hat{\omega}) = 2\hat{k}\hat{Q}/\hat{\omega}$ is called the *shunt impedance*. The *quality factor* \hat{Q} describes the decay time

$$\hat{\tau} = 2\hat{Q}/\hat{\omega},$$

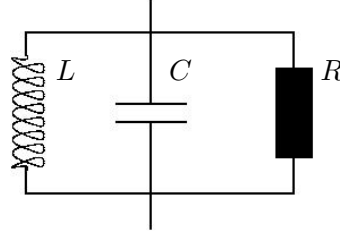


Fig. 12: Equivalent circuit model of the impedance of one mode

the resonance bandwidth

$$\Delta\hat{\omega} = \omega/\hat{Q},$$

with $|\hat{Z}_{\parallel}(\hat{\omega})/\hat{Z}_{\parallel}(\hat{\omega} \pm \Delta\hat{\omega}/2)|^2 \approx 2$, and the energy loss per unit time

$$\hat{P} = \hat{\omega}\hat{\mathcal{W}}/\hat{Q}.$$

The last relation is used to determine the quality factor by perturbation theory: the energy loss (without beam) is caused by wall losses; as a good approximation these can be calculated from the fields obtained for the mode with infinite conductivity. If \hat{H}_t is the magnetic field tangential to the surface, the total power dissipated into the wall is given by a surface integral

$$\hat{P} = \frac{1}{2} \int_{\partial V} \text{Re}\{\hat{\mathbf{E}}_s \times \hat{\mathbf{H}}^*\} \cdot d\mathbf{A} = \frac{1}{2} \int_{\partial V} \sqrt{\frac{\hat{\omega}\mu}{2\kappa}} |\hat{\mathbf{H}}|^2 dA$$

where $\hat{\mathbf{E}}_s = Z_s \mathbf{n} \times \hat{\mathbf{H}}$ is the tangential component of the electric field on the surface, with surface impedance $Z_s = \sqrt{i\hat{\omega}\mu/\kappa}$ for conductivity κ .

5 Instabilities

5.1 Equation of motion

In the previous section the properties of the wake potential and the related impedance has been discussed in detail. Now the effect on the beam motion will be studied. The kick on a test charge due to a transverse dipole wake is

$$\vec{\theta}(s) = \frac{e}{E} q W_{\perp}^{(1)}(s) \vec{r},$$

where E is the beam energy, q the charge of the bunch with transverse offset \vec{r} .

In the rigid bunch approximation the transverse equation of a bunch in a storage can be written as:

$$\frac{d^2}{ds^2} y(s) + \left(\frac{\omega_{\beta}}{c}\right)^2 y(s) = 0,$$

where s is the longitudinal position in the storage ring, y is a transverse coordinate of the bunch and ω_{β} the betatron frequency.

In order to include wakefield effects one has to modify the above equation [3]:

$$\frac{d^2}{ds^2} y(s) + \left(\frac{\omega_{\beta}}{c}\right)^2 y(s) = \frac{e}{mc^2 \gamma} q \sum_{n=0}^{\infty} \frac{1}{C} y(s - nC) W_{\perp}^{(1)}(nC),$$

where C is the circumference of the storage ring and γ the relativistic γ -factor. The right hand side of the equation is a sum of all the wakefield kicks during each turn in the storage ring.

An ansatz for the solution of the above equation is

$$y(s) \sim \exp(-i \Omega s/c),$$

with the complex frequency Ω :

$$\Omega = \omega_\beta + i \frac{1}{\tau},$$

including the betatron frequency ω_β and the growth or damping rate $1/\tau$.

The ansatz leads to a relation for the complex frequency Ω :

$$\Omega^2 - \omega_\beta^2 = -i \frac{e q}{m c^2 \gamma} \frac{c}{T_0^2} \sum_{p=-\infty}^{\infty} Z_{\perp}^{(1)}(\Omega + p\omega_0).$$

The transformation from the time domain picture to the frequency picture is based on the relation:

$$\sum_{n=0}^{\infty} \exp(i n \Omega T_0) W_{\perp}^{(1)}(n C) = \frac{i}{T_0} \sum_{p=-\infty}^{\infty} Z_{\perp}^{(1)}(\Omega + p\omega_0),$$

which allows to replace the wake potential with the impedance $Z_{\perp}^{(1)}$. T_0 is the revolution time in the storage ring.

If one further assumes that Ω does not deviate much from ω_β ($\Omega + \omega_\beta \approx 2\omega_\beta$) one obtains an relation for the betatron tune shift and the growth rate with the transverse impedance:

$$\Omega - \omega_\beta = -i \frac{1}{2\omega_\beta} \frac{e q}{m c^2 \gamma} \frac{c}{T_0^2} \sum_{p=-\infty}^{\infty} Z_{\perp}^{(1)}(\omega_\beta + p\omega_0).$$

The imaginary part is contributing to a mode frequency shift $\Delta\Omega = \text{Re}(\Omega - \omega_\beta)$, while the real part of the impedance corresponds to a growth rate $1/\tau = \text{Im}(\Omega - \omega_\beta)$:

$$\tau^{-1} = - \frac{1}{2\omega_\beta} \frac{e q}{m c^2 \gamma} \frac{c}{T_0^2} \sum_{p=-\infty}^{\infty} \text{Re}(Z_{\perp}^{(1)})(\omega_\beta + p\omega_0).$$

This demonstrates how the impedance can be use to calculate instability growth rates for a simplified model of transverse rigid bunch motion. In the next section a two macro particle is used to get a basic understanding of a head tail instability in an storage ring.

5.2 Head tail instability

In the previous section the bunch was modelled just as a rigid bunch without an internal structure. Now it is assumed that the bunch consists of two parts, a head and a tail as show in Fig. 13. This two particle model can be used to included synchrotron oscillations.

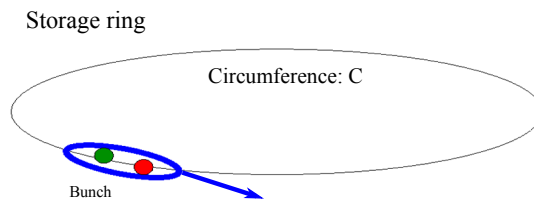


Fig. 13: Headtail model of a bunch in a storage ring.

The starting point is again the kick of the head particle on the tail particle of the bunch: The kick on a test charge due to a transverse dipole wake is

$$\theta_{tail} = \frac{e}{E} \frac{q}{2} \mathcal{W}_{\perp} y_{head}$$

where E is the beam energy, q the charge of the bunch with transverse offset y_{head} of the head. \mathcal{W}_{\perp} is the effective wake of the head of the bunch acting on the tail of the bunch.

The equation of motion for the two particles are:

$$y''_1 + \left(\frac{\omega_{\beta}}{c}\right)^2 y_1 = 0$$

for the head particle and

$$y''_2 + \left(\frac{\omega_{\beta}}{c}\right)^2 y_2 = \frac{N r_0}{2\gamma C} \mathcal{W}_{\perp} y_1$$

for the tail particle, where

$$r_0 = \frac{1}{4\pi\epsilon_0} \frac{e^2}{m_0 c^2} = 2.818 \cdot 10^{-15} \text{ m}$$

is the classical radius of the electron and N is the bunch population. $N/2$ electrons are in the head. The positions of the head and the tail are exchanged after one synchrotron oscillation period as illustrated in Fig. 14. Therefor the above equation of motion are only valid for one half of a period of synchrotron oscillations. For the second half of the synchrotron oscillation period the indices's have to interchanged.

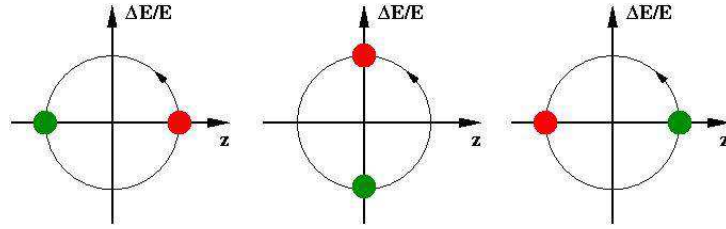


Fig. 14: Synchrotron oscillation of the head and tail macro particles in the bunch.

The equation of motions can also be rewritten in a complex phasor notion for both particles with the index 1 and 2 [3]:

$$\tilde{y}_{1,2} = y_{1,2} + i \frac{c}{\omega_{\beta}} y'_{1,2}$$

For the first half of the synchrotron oscillation period the following relations holds:

$$\begin{pmatrix} \tilde{y}_1 \\ \tilde{y}_2 \end{pmatrix}_{s=cT_s/2} = \exp(-i \omega_{\beta} T_s/2) \begin{pmatrix} 1 & 0 \\ i \Upsilon & 1 \end{pmatrix} \begin{pmatrix} \tilde{y}_1 \\ \tilde{y}_2 \end{pmatrix}_{s=0},$$

where the wakefield effect is now presented with the parameter Υ , defined as:

$$\Upsilon = \frac{\pi N r_0 c^2}{4\gamma C \omega_{\beta} \omega_s} \mathcal{W}_{\perp}.$$

For one complete synchrotron period one obtains now the relation

$$\begin{pmatrix} \tilde{y}_1 \\ \tilde{y}_2 \end{pmatrix}_{s=cT_s} = \exp(-i \omega_{\beta} T_s) \begin{pmatrix} 1 & i \Upsilon \\ 0 & 1 \end{pmatrix} \begin{pmatrix} 1 & 0 \\ i \Upsilon & 1 \end{pmatrix} \begin{pmatrix} \tilde{y}_1 \\ \tilde{y}_2 \end{pmatrix}_{s=0}.$$

Stability requires pure imaginary eigenvalues of the product matrix which can be translated into a criteria for the parameter Υ :

$$\Upsilon < 2.$$

For a known effective wakefield \mathcal{W}_\perp this can be directly translated into an limit for the bunch population which will be stable with respect to head tail instabilities:

$$N < \frac{2\gamma C\omega_\beta\omega_s}{\pi N r_0 c^2} \frac{1}{\mathcal{W}_\perp}.$$

5.3 Ion trapping

Finally, the effect of ion trapping will be discussed, which can result in an increased beam emittance, betatron tune shifts and reduced beam lifetime. The effect of the ion cloud on the beam can be modelled as a broad band resonator wake field [25]. One can apply the classical theory of instabilities to obtain stability criteria with respect to ion effects. Nevertheless, it is interesting to have a simple criteria at hand to know whether one can expect trapped ions in a beam. This was already analyzed by Kohaupt in 1971 [26] for the storage ring DORIS at DESY.

The residual gas density d_{gas} at room temperature (300 K) can be calculated from vacuum pressure:

$$d_{gas} = \frac{p_{gas}}{R_{gas}} \frac{N_{Avo}}{300 \text{ K}} = 24.14 \cdot 10^6 \text{ cm}^{-3},$$

where the numbers have been calculated for $p_{gas} = 1 \cdot 10^{-9}$ mbar. $R_{gas} = 8.31447 \text{ J/(K mol)}$ is the general gas constant and $N_A = 6.0221367 \cdot 10^{23}$ is the Avogadro number.

Assuming now a typical cross section of 2 Mbarn ($2 \cdot 10^{-18} \text{ cm}^2$) for the ionization process, one obtains an ion density of

$$\lambda_{ion} = d_{gas} \sigma_{ion} N_0 \approx 2 \text{ Mbarn } d_{gas} N_0,$$

where N_0 is the bunch population. After the passage of one bunch with a bunch population of $5 \cdot 10^9$ the ion density is already 0.24 ions/cm or 230 ions/cm after the passage of 960 bunches, which is one of the filling modes of the synchrotron radiation facility PETRA III at DESY.

The bunch train in a storage ring is acting as sequence of quadrupole lenses on the ion beam. In a linear approximation the interaction of the bunch with the ion can be presented by a matrix:

$$M = \begin{pmatrix} 1 & L_b \\ 0 & 1 \end{pmatrix} \begin{pmatrix} 1 & 0 \\ -a & 1 \end{pmatrix},$$

where $L_b = c \Delta t$ is the bunch spacing, and

$$a = N_b \frac{2 r_p}{\sigma_y (\sigma_x + \sigma_y)} \frac{1}{A}$$

is the linear force of the beam on the ion. N_b is the bunch population, $r_p = 1.535 \cdot 10^{-18} \text{ m}$, σ_x , σ_y are the transverse rms beam dimensions and A is the mass number of the ion. For CO and N_2 the mass number is $A = 28$, while for water $A = 18$. The ion motion will be only stable if the trace of the matrix M is smaller than 2, or $\text{Tr}(M) = 2 - a L_b < 2$. The ion will be trapped, when the mass number A is larger than a critical mass number A_c :

$$A > A_c = N_b L_b \frac{r_p}{2 \sigma_y (\sigma_x + \sigma_y)}.$$

Appendix A: Eigenmodes of a closed cavity

We consider a (simply connected) cavity volume V_c , with perfectly conducting walls (boundary ∂V_c) and without current density. We search for time-harmonic eigensolutions, which can be written as

$$\begin{aligned}\mathbf{E}(\mathbf{r}, t) &= \hat{\mathbf{E}}(\mathbf{r}) \cos(\hat{\omega}t), \\ \mathbf{B}(\mathbf{r}, t) &= \hat{\mathbf{B}}(\mathbf{r}) \sin(\hat{\omega}t),\end{aligned}$$

where $\hat{\mathbf{E}}$ and $\hat{\mathbf{B}}$ are the eigenfields and $\hat{\omega}$ the (angular) eigenfrequencies. Substituting these into Maxwell's equations gives

$$\begin{aligned}\nabla \varepsilon \hat{\mathbf{E}} &= \hat{\rho}, \\ \nabla \times \hat{\mathbf{E}} &= -\hat{\omega} \hat{\mathbf{B}}, \\ \nabla \hat{\mathbf{B}} &= 0, \\ \nabla \times \mu^{-1} \hat{\mathbf{B}} &= -\hat{\omega} \varepsilon \hat{\mathbf{E}}.\end{aligned}$$

We apply the operator $\nabla \times \mu^{-1}$ to the first curl equation and use the second curl equation to eliminate the magnetic flux density, thus obtaining the eigenproblem

$$\varepsilon^{-1} \nabla \times \mu^{-1} \nabla \times \hat{\mathbf{E}} = \hat{\lambda} \hat{\mathbf{E}},$$

with the eigenvalues $\hat{\lambda} = \hat{\omega}^2$ and the boundary condition $\mathbf{n} \times \hat{\mathbf{E}} = \mathbf{0}$. The operator $\varepsilon^{-1} \nabla \times \mu^{-1} \nabla \times$ is self-adjoint⁴ with scalar product

$$\langle \mathbf{A}, \mathbf{B} \rangle = \frac{1}{2} \int_{V_c} \varepsilon \mathbf{A} \cdot \mathbf{B} \, dV.$$

Therefore the problem has an infinite number of discrete real eigenvalues and a complete orthogonal system of eigenvectors,

$$\langle \hat{\mathbf{E}}_\xi, \hat{\mathbf{E}}_\tau \rangle = \hat{\mathcal{W}}_\xi \delta_{\xi\tau},$$

where $\hat{\mathcal{W}}_\xi$ is the electromagnetic field energy of mode ξ . The eigenvalues $\hat{\lambda}$ are non-negative so that all eigenfrequencies $\hat{\omega}$ are real.⁵

There are obviously two types of eigensolutions:

$$\begin{aligned}\hat{\omega} &= 0, & \hat{\omega} &\neq 0, \\ \nabla \varepsilon \hat{\mathbf{E}} &\neq 0, & \nabla \varepsilon \hat{\mathbf{E}} &= 0, \\ \nabla \times \hat{\mathbf{E}} &= 0, & \nabla \times \hat{\mathbf{E}} &= -\hat{\omega} \hat{\mathbf{B}}, \\ \hat{\mathbf{B}} &\equiv 0, & \hat{\mathbf{B}} &\neq 0.\end{aligned}$$

Eigenfields for $\hat{\omega} = 0$ are curl-free and are just solutions to the electrostatic problem for any source distribution $\hat{\rho}$ and the boundary condition $\mathbf{n} \times \hat{\mathbf{E}} = \mathbf{0}$. Oscillating eigenfields are free of divergence; this is a consequence of Maxwell's second curl equation.

In Appendix B we use the property that any linear combination of eigensolutions with $\hat{\omega} = 0$ is orthogonal to any linear combination of oscillating eigenfields.

⁴ The property $\langle \varepsilon^{-1} \nabla \times \mu^{-1} \nabla \times \mathbf{A}, \mathbf{B} \rangle = \langle \mathbf{A}, \varepsilon^{-1} \nabla \times \mu^{-1} \nabla \times \mathbf{B} \rangle$ can be shown with help of the identity $\nabla[\mathbf{A} \times \mu^{-1} \nabla \times \mathbf{B} - \mathbf{B} \times \mu^{-1} \nabla \times \mathbf{A}] = \mathbf{B} \times \nabla \times \mu^{-1} \nabla \times \mathbf{A} - \mathbf{A} \times \nabla \times \mu^{-1} \nabla \times \mathbf{B}$ and the divergence theorem. The left-hand side gives a surface integral that is zero because of the boundary conditions. The right-hand side corresponds to the assertion.

⁵ This property can be shown by using the identity $\nabla[\hat{\mathbf{E}} \times \mu^{-1} \nabla \times \hat{\mathbf{E}}] = \mu^{-1}(\nabla \times \hat{\mathbf{E}})^2 - \hat{\mathbf{E}} \nabla \times \mu^{-1} \nabla \times \hat{\mathbf{E}}$ and the divergence theorem. The left-hand side gives a surface integral that is zero because of the boundary conditions. The volume integral of the first term on the right-hand side is non-negative; the integral of the second term gives $-2\hat{\lambda}\hat{\mathcal{W}}$. As $\hat{\mathcal{W}}$ is positive, $\hat{\lambda}$ cannot be negative.

Appendix B: Wake of a closed cavity

We consider a (simply connected) cavity volume V_c of arbitrary shape, with perfectly conducting walls, that is located between the planes $z = 0$ and $z = L$. It is traversed by a point particle with charge q_1 , offset (x_1, y_1) and velocity $v = c$. The stimulating charge and current density are

$$\begin{aligned}\rho(\mathbf{r}, t) &= q_1 \delta(x - x_1) \delta(y - y_1) \delta(z - ct), \\ \mathbf{j}(\mathbf{r}, t) &= c \mathbf{e}_z \rho(\mathbf{r}, t).\end{aligned}$$

We use the complete orthogonal system of eigensolutions to describe the time-dependent electric field:

$$\mathbf{E}(\mathbf{r}, t) = \sum_{\nu \in C} \hat{a}_\nu(t) \hat{\mathbf{E}}_\nu(\mathbf{r}),$$

where ν is the mode index, C is the set of all indexes and $\hat{a}_\nu(t)$ are the time-dependent coefficients. As in the main text, we shall write all mode-specific quantities with a hat and omit the index ν . We solve Maxwell's equations

$$\begin{aligned}\nabla \varepsilon \mathbf{E} &= \rho, \\ \nabla \times \mathbf{E} &= -\frac{\partial}{\partial t} \mathbf{B}, \\ \nabla \mathbf{B} &= 0, \\ \nabla \times \mu^{-1} \mathbf{B} &= \mathbf{J} + \varepsilon \frac{\partial}{\partial t} \mathbf{E}\end{aligned}$$

by applying the operator $\varepsilon^{-1} \nabla \times \mu^{-1}$ to the first curl equation and eliminating the magnetic flux density with the help of the second curl equation:

$$\varepsilon^{-1} \nabla \times \mu^{-1} \nabla \times \mathbf{E} = -\varepsilon^{-1} \frac{\partial}{\partial t} \mathbf{J} - \frac{\partial^2}{\partial t^2} \mathbf{E}.$$

By using the modal expansion and the eigenmode equation, we obtain

$$\sum_{\nu \in C} \hat{a}(t) \hat{\omega}^2 \hat{\mathbf{E}} = -\varepsilon^{-1} \frac{\partial}{\partial t} \mathbf{J} - \frac{\partial^2}{\partial t^2} \sum_{\nu \in C} \hat{a}(t) \hat{\mathbf{E}}.$$

This set of scalar equations can be decoupled by applying the operator $\langle \hat{\mathbf{E}}_\xi, \dots \rangle$ to both sides and using the orthogonality condition:

$$\hat{a}_\xi(t) \hat{\omega}_\xi^2 \hat{\mathcal{W}}_\xi = -\varepsilon^{-1} \frac{\partial}{\partial t} \langle \hat{\mathbf{E}}_\xi, \mathbf{J} \rangle - \frac{\partial^2}{\partial t^2} \hat{a}_\xi(t) \hat{\mathcal{W}}_\xi.$$

Finally, we substitute the Dirac current density and suppress the index, to arrive at

$$\left(\hat{\omega}^2 + \frac{\partial^2}{\partial t^2} \right) \hat{a}(t) = \frac{-1}{\hat{\mathcal{W}}_\varepsilon} \frac{\partial}{\partial t} \langle \hat{\mathbf{E}}, \mathbf{J} \rangle = -\frac{cq_1}{2\hat{\mathcal{W}}} \frac{\partial}{\partial t} \hat{E}(x_1, y_1, ct).$$

This ordinary differential equation can be solved⁶ to give

$$\hat{a}(t) = \frac{-q}{\sqrt{\hat{\mathcal{W}}}} \operatorname{Re} \{ \hat{v}^*(x_1, y_1, ct) \exp(i \hat{\omega} t) \}$$

with

$$v(x, y, z) = \frac{1}{2\sqrt{\hat{\mathcal{W}}}} \int_{-\infty}^z \hat{E}_z(x, y, s) \exp(i \hat{\omega} s/c) ds$$

⁶ The causal solution of $\ddot{a} + \omega^2 a = \dot{b}$ is $a(t) = \operatorname{Re} \{ \int_{-\infty}^t b(\tau) \exp(i \omega(t - \tau)) d\tau \}$.

and

$$\frac{\partial}{\partial z} v(x, y, z) = \frac{1}{2\sqrt{\hat{\mathcal{W}}}} \hat{E}_z(x, y, z) \exp(i\hat{\omega}z/c).$$

The longitudinal wake function is the sum over all modes,

$$w_{\parallel}(x_1, y_1, x_2, y_2, s) = \sum_{\nu \in C} \hat{w}_{\parallel}(x_1, y_1, x_2, y_2, s),$$

with the ‘per-mode’ contributions

$$\begin{aligned} \hat{w}_{\parallel}(x_1, y_1, x_2, y_2, s) &= \frac{1}{q_1} \int_{-\infty}^{\infty} \hat{a}\left(\frac{z+s}{c}\right) \hat{E}_z(x_2, y_2, z) dz \\ &= \frac{-1}{\sqrt{\hat{\mathcal{W}}}} \int_{-\infty}^{\infty} \operatorname{Re} \left\{ \hat{v}^*(x_1, y_1, z+s) \exp\left(i\hat{\omega} \frac{z+s}{c}\right) \right\} \hat{E}_z(x_2, y_2, z) dz \\ &= -2 \operatorname{Re} \left\{ \exp(i\hat{\omega}s/c) \int_{-\infty}^{\infty} \hat{v}^*(x_1, y_1, z+s) \frac{\partial}{\partial z} v(x_2, y_2, z) dz \right\}. \end{aligned}$$

None of these terms is causal, i.e. $\hat{w}_{\parallel}(x_1, y_1, x_2, y_2, s < 0) \neq 0$, but the sum has to be! In the following we use causality to find the simplified representation of the longitudinal wake function

$$w_{\parallel}(x_1, y_1, x_1, y_1, s > 0) = -2 \sum_{\hat{\omega} \neq 0} \hat{k}(x_1, y_1) \cos(\hat{\omega}s/c)$$

for $x_1 = x_2$ and $y_1 = y_2$, where $\hat{k}(x_1, y_1)$ is the longitudinal per-mode loss parameter, as defined in the main text. We therefore split the summation over all modes into the components

$$\begin{aligned} w_{\parallel d}(x_1, y_1, x_2, y_2, s) &= \sum_{\hat{\omega}=0} \hat{w}_{\parallel}(x_1, y_1, x_2, y_2, s), \\ w_{\parallel c}(x_1, y_1, x_2, y_2, s) &= \sum_{\hat{\omega} \neq 0} \hat{w}_{\parallel}(x_1, y_1, x_2, y_2, s) \end{aligned}$$

and use the causality relation

$$w_{\parallel d}(x_1, y_1, x_2, y_2, s < 0) + w_{\parallel c}(x_1, y_1, x_2, y_2, s < 0) = 0$$

together with the anti-symmetry of the non-resonant part,

$$w_{\parallel d}(x_1, y_1, x_2, y_2, s) = -w_{\parallel d}(x_2, y_2, x_1, y_1, -s)$$

proved in (A) below, to eliminate $w_{\parallel d}$, yielding

$$w_{\parallel}(x_1, y_1, x_2, y_2, s > 0) = w_{\parallel c}(x_1, y_1, x_2, y_2, s) + w_{\parallel c}(x_2, y_2, x_1, y_1, -s).$$

To get the simplified representation for $x_1 = x_2$ and $y_1 = y_2$, we have to show that the condition

$$(B) \quad \hat{w}_{\parallel}(x_1, y_1, x_1, y_1, s) + \hat{w}_{\parallel}(x_1, y_1, x_1, y_1, -s) = -2\hat{k}(x_1, y_1) \cos(\hat{\omega}s/c)$$

is fulfilled for eigenmodes with $\hat{\omega} \neq 0$.

We will now prove (A) and (B).

(A) For *non-oscillating modes* ($\hat{\omega} = 0$), the normalized voltage integrals $\hat{v}(x, y, z)$ are real and the contribution per mode is

$$\hat{w}_{\parallel}(x_1, y_1, x_2, y_2, s) = -2 \int_{-\infty}^{\infty} \hat{v}(x_1, y_1, z+s) \frac{\partial}{\partial z} \hat{v}(x_2, y_2, z) dz.$$

Therefore the required symmetry is fulfilled:

$$\begin{aligned}
\hat{w}_{\parallel}(x_1, y_1, x_2, y_2, s) &= -2 \int_{-\infty}^{\infty} \hat{v}(x_1, y_1, z + s) \frac{\partial}{\partial z} \hat{v}(x_2, y_2, z) dz \\
&= 2 \int_{-\infty}^{\infty} \hat{v}(x_2, y_2, z) \frac{\partial}{\partial z} \hat{v}(x_1, y_1, z + s) dz \\
&= 2 \int_{-\infty}^{\infty} \hat{v}(x_2, y_2, z - s) \frac{\partial}{\partial z} \hat{v}(x_1, y_1, z) dz = -\hat{w}_{\parallel}(x_2, y_2, x_1, y_1, -s).
\end{aligned}$$

The physical meaning of this symmetry is that the energy transfer from particle 1 to particle 2 (by $\hat{w}_{\parallel}(x_1, y_1, x_2, y_2, s)$) plus the reverse energy transfer (by $\hat{w}_{\parallel}(x_2, y_2, x_1, y_1, -s)$) is zero. This is obvious as no energy is left to the non-resonant mode after both particles have departed the volume. The voltage $\hat{v}(x, y, z)$ is zero for $z < 0$ before the source q_1 entered the cavity and, as the eigensolution is curl-free, it is zero for $z \geq L$. Therefore $\hat{w}_{\parallel}(\dots, s) = 0$ for $|s| > L$. Two particles can interact only through non-oscillating modes if they are simultaneously in the cavity at any time.

(B) The normalized voltage integral for *oscillating modes* ($\omega \neq 0$) does not depend on z after q_1 has left the cavity:

$$v(x, y, z > L) = \frac{1}{2\sqrt{\mathcal{W}}} \int_{-\infty}^L \hat{E}_z(x, y, s) \exp(i\hat{\omega}s/c) ds = v(x, y).$$

Therefore the following integral relation can be derived:

$$\begin{aligned}
\hat{v}^*(x_1, y_1) \hat{v}(x_2, y_2) &= \int_{-\infty}^{\infty} \frac{\partial}{\partial z} \{ \hat{v}^*(x_1, y_1, z + s) \hat{v}(x_2, y_2, z) \} dz \\
&= \int_{-\infty}^{\infty} \hat{v}(\dots_2, z) \frac{\partial}{\partial z} \hat{v}^*(\dots_1, z + s) dz + \int_{-\infty}^{\infty} \hat{v}^*(\dots_1, z + s) \frac{\partial}{\partial z} \hat{v}(\dots_2, z) dz \\
&= \int_{-\infty}^{\infty} \hat{v}(\dots_2, z - s) \frac{\partial}{\partial z} \hat{v}^*(\dots_1, z) dz + \int_{-\infty}^{\infty} \hat{v}^*(\dots_1, z + s) \frac{\partial}{\partial z} \hat{v}(\dots_2, z) dz.
\end{aligned}$$

This relation is needed to prove the symmetry:

$$\begin{aligned}
&\hat{w}(x_1, y_1, x_2, y_2, s) \\
&= -2 \operatorname{Re} \left\{ \exp(i\hat{\omega}s/c) \int_{-\infty}^{\infty} \hat{v}^*(x_1, y_1, z + s) \frac{\partial}{\partial z} \hat{v}(x_2, y_2, z) dz \right\} \\
&= -2 \operatorname{Re} \left\{ \exp(i\hat{\omega}s/c) \left[\hat{v}^*(x_1, y_1) \hat{v}(x_2, y_2) - \int_{-\infty}^{\infty} \hat{v}^*(\dots_1, z + s) \frac{\partial}{\partial z} \hat{v}(\dots_2, z) dz \right] \right\} \\
&= -2 \operatorname{Re} \{ \exp(i\hat{\omega}s/c) \hat{v}^*(x_1, y_1) \hat{v}(x_2, y_2) \} - \hat{w}(x_2, y_2, x_1, y_1, -s).
\end{aligned}$$

With $x_1 = x_2$ and $y_1 = y_2$, we find that

$$\hat{w}(x_1, y_1, x_1, y_1, s) + \hat{w}(x_1, y_1, x_1, y_1, -s) = -2\hat{k}(x_1, y_1) \cos(\hat{\omega}s/c),$$

where $\hat{k}(x_1, y_1) = |\hat{v}(x_1, y_1)|^2$; in particular, for the origin,

$$\hat{w}(x_1, y_1, x_1, y_1, 0) = -\hat{k}(x_1, y_1).$$

Acknowledgments

First and foremost I would like to thank the audience of my lecture for their interest. I am also grateful to the CAS team for their organizational efforts and patience. Last but not least I am gratefully acknowledging the collaboration with Martin Dohlus on a previous CERN school which is the basis for this contributions to the proceedings.

References

- [1] T. Weiland and R. Wanzenberg, Wakefields and impedances, Proceedings of US–CERN School (Hilton Head, 1990), edited by M. Dienes, M. Month and S. Turner (Springer, Berlin, 1992), http://dx.doi.org/10.1007/3-540-55250-2_26.
- [2] M. Dohlus and R. Wanzenberg, An Introduction to Wake Fields and Impedances, Proceedings of the CERN Accelerator School: Intensity Limitations in Particle Beams, Geneva, 2015, edited by W. Herr, CERN-2017-006-SP.
- [3] A.W. Chao, *Physics of Collective Beam Instabilities in High Energy Accelerators* (Wiley, New York, 1993).
- [4] B.W. Zotter and S.A. Kheifets, *Impedances and Wakes in High-Energy Particle Accelerators* (World Scientific, Singapore, 1998), <http://dx.doi.org/10.1142/3068>.
- [5] K.Y. Ng, *Physics of Intensity Dependent Beam Instabilities* (World Scientific, Hackensack, 2005), <http://dx.doi.org/10.1142/5835>.
- [6] A. Wolski, *Beam Dynamics in High Energy Particle Accelerators* (Imperial College Press, London, 2014), <http://dx.doi.org/10.1142/p899>.
- [7] J.D. Jackson, *Classical Electrodynamics*, 2nd edition (Wiley, New York, 1975).
- [8] O. Brüning, H. Burkhardt and S. Myers, *Prog. Part. Nucl. Phys.* **67** (2012) 705, <http://dx.doi.org/10.1016/j.pnpnp.2012.03.001>.
- [9] *LEP Design Report. Vol. 2: The LEP Main Ring*, CERN-LEP-84-01 (1984).
- [10] K. Balewski *et al.* (eds.), PETRA III: A Low Emittance Synchrotron Radiation Source, DESY 2004-035 (February 2004).
- [11] *MAFIA User Guide*, CST – Computer Simulation Technology AG, Bad Nauheimer Str. 19, 64289 Darmstadt, Germany.
- [12] *CST Studio Suite*, CST – Computer Simulation Technology AG, Bad Nauheimer Str. 19, 64289 Darmstadt, Germany.
- [13] T. Weiland, Transient electromagnetic fields excited by bunches of charged particles in cavities of arbitrary shape, Proceedings of the 11th International Conference on High-Energy Accelerators, Geneva, 1980 (Birkhäuser, Basel, 1980), pp. 570–575, http://dx.doi.org/10.1007/978-3-0348-5540-2_75.
- [14] T. Weiland, *Part. Accel.* **15** (1984) 245.
- [15] A. Piwinski, Longitudinal and transverse wake fields in flat vacuum chambers, DESY 84/097 (October 1984).
- [16] K. Steinigke, *Frequenz* **44** (1990), 4–8, <http://dx.doi.org/10.1515/freq.1990.44.1.2>.
- [17] M. Dohlus, M. I. Ivanian and V. M. Tsakanov, Surface roughness study for the TESLA-FEL, DESY-TESLA-FEL-2000-26, <http://dx.doi.org/10.3204/PUBDB-2018-04074>.
- [18] A. Chao, Beam dynamics with high intensity, Proceedings of the CERN Accelerator School: Intensity Limitations in Particle Beams, Geneva, 2015, edited by W. Herr, CERN-2017-006-SP
- [19] W.K.H. Panofsky and W.A. Wenzel, *Rev. Sci. Instrum.* **27** (1956), 967, <http://dx.doi.org/10.1063/1.1715427>.
- [20] I. Zagorodnov, K. Bane and G. Stupakov, *Phys. Rev. ST Accel. Beams* **18** (2015), 104401, <http://dx.doi.org/10.1103/physrevstab.18.104401>.
- [21] I. Zagorodnov and T. Weiland, *Phys. Rev. ST Accel. Beams* **8** (2005), 042001, <http://dx.doi.org/10.1103/physrevstab.8.042001>.
- [22] I. Zagorodnov, ECHO 2D, http://www.desy.de/~zagor/WakefieldCode_ECHOz/.
- [23] T. Weiland and I. Zagorodnov, *The Short-Range Transverse Wake Function for TESLA Accelerating Structure*, TESLA Report 2003-19, DESY (2003).

- [24] T. Weiland and B. Zotter, *Part. Accel.* **11** (1981), 143.
- [25] L. Wang, Y. Cai, T. O. Raubenheimer, and H. Fukuma, Suppression of beam-ion instability in electron rings with multibunch train beam fillings, *Phys. Rev. ST Accel. Beams* **14** (2011), 084401, <https://doi.org/10.1103/PhysRevSTAB.14.084401>.
- [26] R.D. Kohaupt, Mechanismus der Ionenabsaugung im Elektron-Positron-Speicherring (DORIS), Internal Report, DESY HI-71/2, Dezember 1971.